Redox Biology 26 (2019) 101283

Contents lists available at ScienceDirect

Redox Biology

journal homepage: www.elsevier.com/locate/redox

Research Paper

Oxidative inactivation of amyloid beta-degrading proteases by cholesterol-enhanced mitochondrial stress

Cristina de Dios[a,b,c], Isabel Bartolessis[a], Vicente Roca-Agujetas[a,c], Elisabet Barbero-Camps[a], Montserrat Mari[a], Albert Morales[a], Anna Colell[a,c,*]

[a] Department of Cell Death and Proliferation, Institut D'Investigacions Biomèdiques de Barcelona, Consejo Superior de Investigaciones Científicas (CSIC), Institut D'Investigacions Biomèdiques August Pi I Sunyer (IDIBAPS), Barcelona, Spain
[b] Departament de Biomedicina, Facultat de Medicina, Universitat de Barcelona, Barcelona, Spain
[c] Centro de Investigación Biomédica en Red Sobre Enfermedades Neurodegenerativas (CIBERNED), Spain

ARTICLE INFO

Keywords:
Alzheimer's disease
Aβ proteolytic clearance
GSH
2-Hydroxypropyl-β-cyclodextrin
Neprilysin
Insulin-degrading enzyme
Antioxidant

ABSTRACT

Familial early-onset forms of Alzheimer's disease (AD) are linked to overproduction of amyloid beta (Aβ) peptides, while decreased clearance of Aβ is the driving force leading to its toxic accumulation in late-onset (sporadic) AD. Oxidative modifications and defective function have been reported in Aβ-degrading proteases such as neprilysin (NEP) and insulin-degrading enzyme (IDE). However, the exact mechanisms that regulate the proteolytic clearance of Aβ and its deficits are largely unknown. We have previously showed that cellular cholesterol loading, by depleting the mitochondrial GSH (mGSH) content, stimulates Aβ-induced mitochondrial oxidative stress and promotes AD-like pathology in APP-PSEN1-SREBF2 mice. Here, using the same AD mouse model we examined whether cholesterol-enhanced mitochondrial oxidative stress affects NEP and IDE function. We found that brain extracts from APP-PSEN1-SREBF2 mice displayed increased presence of oxidatively modified forms of NEP and IDE, associated with impaired enzymatic activities. Both alterations were substantially recovered after an *in vivo* treatment with the cholesterol-lowering agent 2-hydroxypropyl-β-cyclodextrin. The recovery of the proteolytic activity after treatment was accompanied with a significant reduction of Aβ levels. Supporting these results, cholesterol-enriched SH-SY5Y cells were more sensitive to Aβ-induced impairment of IDE and NEP function *in vitro*. The rise of cellular cholesterol also stimulated the extracellular release of IDE by an unconventional autophagy-coordinated mechanism. Recovery of depleted pool of mGSH in these cells not only prevented the detrimental effect of Aβ on intracellular AβDPs activities but also had an impact on extracellular IDE levels and function, stimulating the extracellular Aβ degrading activity. Therefore, changes in brain cholesterol levels by modifying the mGSH content would play a key role in IDE and NEP-mediated proteolytic elimination of Aβ peptides and AD progression.

1. Introduction

Increased amyloid β (Aβ) load has been consistently linked to the onset and progression of Alzheimer's disease (AD) [1]. Aβ is produced in normal individuals by β- and γ-secretase-mediated cleavage of the amyloid precursor protein (APP); however, under certain circumstances the molecule accumulates to above optimal concentrations leading to its self-association into neurotoxic assemblies.

All mutations causing familial type of AD occur in genes that codify for proteins related to Aβ generation, such us APP and presenilin-1 and -2, the catalytic subunits of the γ-secretase complex, resulting in enhanced amyloidogenic processing. In contrast, the quantification of the rates of Aβ synthesis and clearance within the cerebrospinal fluid (CSF) [2], indicates that Aβ accumulation in sporadic AD patients is mainly due to significant defects in the clearance of the peptide [3].

Several processes operating simultaneously have been described in the elimination of cerebral Aβ, including passive and active transport through the blood brain barrier, interstitial fluid bulk-flow clearance, and proteolytic degradation mediated by a diverse array of intra and extracellular enzymes, known collectively as Aβ-degrading proteases (AβDPs) [4]. The best characterized AβDPs are neprilysin (NEP) and insulin-degrading enzyme (IDE) [5]; both are zinc-metalloendopeptidases particularly involved in the degradation of monomeric species, although neprilysin has been also described to hydrolyze Aβ oligomers

* Corresponding author. Department of Cell Death and Proliferation, Institut d'Investigacions Biomèdiques de Barcelona, (IIBB-CSIC), Rosselló 160, 08036, Barcelona, Spain.
E-mail address: anna.colell@iibb.csic.es (A. Colell).

https://doi.org/10.1016/j.redox.2019.101283
Received 23 April 2019; Received in revised form 15 July 2019; Accepted 24 July 2019
Available online 25 July 2019
2213-2317/ © 2019 Published by Elsevier B.V. This is an open access article under the CC BY-NC-ND license (http://creativecommons.org/licenses/BY-NC-ND/4.0/).

Abbreviations

AD	Alzheimer's disease
Aβ	amyloid β
AβDPs	Aβ-degrading proteases
ACTB	β-actin
APP	amyloid precursor protein
APOE	apolipoprotein E
CHO:MCD	cholesterol:methyl-β-cyclodextrin complex
EVs	extracellular vesicles
FLOT1	flotillin 1
GSHee	glutathione ethyl ester
4-HNE	4-hydorxynonenal
HP-β-CD	2-hydroxypropil-β-cyclodextrin
IDE	insulin-degrading enzyme
MAP1LC3B/LC3B	microtubule-associated protein 1 light chain 3 B
mGSH	mitochondrial glutathione
NEP	neprilysin
PSEN1	presenilin 1
ROS	reactive oxygen species
SQSTM1/p62	sequestosome 1
SREBF2	sterol regulatory element-binding transcription factor 2
TGS101	tumor susceptibility gene 101

[6]. NEP is a type II membrane-anchored peptidase with its active site on the extracellular side of the plasma membrane. It is mainly expressed in pre-synaptic terminals of neurons [7] but it has been also reported in activated astrocytes and microglia [8,9]. In contrast, IDE is most abundant in the cytosol and once produced by neurons and glial cells [10,11] can be exported to the extracellular space independently of the classical secretory pathway [12,13]. The exact underlying secretion mechanisms remain unknown, but studies indicate that could be at least in part mediated by exosomes [14,15] in coordination with the autophagy-lysosomal pathway [16].

Levels and activity of IDE and NEP decrease in normal human brains as a result of aging and have been shown to inversely correlate with Aβ-related pathology [17–19]. Low expression of NEP has been described in AD brains, especially in high-plaque-bearing areas such as the hippocampus [20]. Changes in AβDPs expression have been also observed under ischemia and hypoxia [8,21], both pathological conditions that have been linked to AD development [22]. Nevertheless, to date our understanding of how AβDPs are regulated in AD is still incomplete. Different studies suggest that the impairment of these proteases in AD brains is caused by post-translational modifications, such as oxidation [8,17,18], and the progressive deposition of aggregated-inactive forms [23]. Evidence indicates that NEP and IDE could be also regulated by cholesterol levels. In retinal pigment epithelial cells, cholesterol enrichment has been shown to enhance Aβ accumulation by down-regulation of NEP expression and activity [24]. Furthermore, the activity of IDE and NEP has been related to *APOE* genotype, being highest in ε2-positive brains and lowest in brains bearing the isoform ε4 [25,26], the major known genetic risk factor for AD [27].

Cholesterol has long been implicated as a contributing factor to AD. High levels of cholesterol have been reported in vulnerable regions of AD brains [28–30] and a wide number of experimental data indicate that the amyloidogenic processing of APP and Aβ aggregation can be regulated by cholesterol levels [31]. Using genetic mouse models of cholesterol loading [sterol regulatory element-binding transcription factor 2 (SREBF2) mice and Niemann-Pick type C1 knock-out mice] together with APP-PSEN1 mice that overexpress SREBF2, we have demonstrated that an excess of cholesterol, particularly in brain mitochondria, by depleting the mitochondrial GSH (mGSH) content, stimulates Aβ-induced mitochondrial oxidative stress and accelerates the onset of the main pathological AD hallmarks [32–34]. Given that both IDE and NEP can be substrates of oxidative damage, in this study we analyze whether changes in cholesterol levels by affecting the mitochondrial antioxidant defense can regulate the expression and activity of both enzymes. We show that strategies directed to preserve mGSH content in cholesterol-enriched cells significantly reduce oxidative modifications in IDE and NEP, protect their function and improve the extracellular Aβ-degrading activity.

2. Materials and methods

2.1. Mice

Breeding pairs of B6C3-Tg (APPswe, PSEN1De9)85Dbo/J (APP-PSEN1) and B6; SJL-Tg (rPEPCKSREBF2)788Reh/J (SREBF2) mice were purchased from The Jackson Laboratory (Maine, USA). APP-PSEN1-SREBF2 were obtained by crossbreeding of APP-PSEN1 and SREBF2 mice and characterized as previously described [34]. Mice were genetically identified by PCR using DNA from ear-tips obtained at the time of weaning (21 d) and following the genotyping protocols provided by the supplier. All the procedures involving animals were approved by the animal care committee of the Universitat de Barcelona and were conducted following the institutional guidelines in accordance with national and international laws and policies. Only male mice were used due to sex-related differences in cholesterol levels observed in APP-PSEN1-SREBF2 mice. In some cases, mice were treated with 2-hydroxypropil-β-cyclodextrin (HP-β-CD 4 g/kg in saline solution), injected subcutaneously at the scruff of neck twice a week for ten weeks.

2.2. Cell culture and treatments

The SH-SY5Y human neuroblastoma cell line (ECACC) was cultured in DMEM supplemented with Ham-F12 (Thermo Fisher Sci., 11330–032), 10% fetal bovine serum (Thermo Fisher Sci., 12484–028) 0.5 mM L-glutamine and 5 μg/ml plasmocin. Cholesterol enrichment was performed by incubation with a cholesterol:methyl-β-cyclodextrin complex (CHO:MCD; containing 50 μg/mL of cholesterol) for 1 h followed by 4 h recovery. Treatment with 4 mM glutathione ethyl ester (GSHee) and/or 5 μM oligomeric Aβ for 24 h was performed when indicated. In some cases, cultured medium from treated cells was collected and cell debris was removed by centrifugation. Then, to concentrate the protein fraction in medium, 1 ml of supernatant was mixed with 10 μg BSA (Bovine serum albumin, Sigma-Aldrich A-4503) and 110 μl of 100% w:v trichloroacetic acid (TCA) on ice for 1 h. Precipitated proteins were pelleted for 5 min at 16,000 *g* at 4 °C, and after rinsed with 500 μl cold acetone, were resuspended for protein analysis.

2.3. Preparation of Aβ peptides

Human Aβ(1–42) hydrochloride salt (Bachem, H-6466) was dissolved to 1 mM in hexafluoroisopropanol (HFIP; Sigma-Aldrich, 10,522–8), aliquoted and stored at −20 °C after HFIP evaporation. For oligomeric assembly, peptides were resuspended to 5 mM in DMSO by sonication, then diluted to 100 μM in phenol red-free DMEM and incubated at 4 °C for 24 h.

2.4. Aβ levels

Levels of human recombinant Aβ(1–42) peptides were determined in duplicate in brain extracts using the colorimetric human Ab42 ELISA kit (Invitrogen KHB3441) following the manufacturer's instructions.

2.5. Mitochondrial isolation

Pure preparations of brain mitochondria were obtained by Percoll gradient centrifugation as described by Yu et al. [35]. First, brains were removed of olfactory bulbs, midbrain, and cerebellum, and were homogenized in 210 mM mannitol, 60 mM sucrose, 10 mM KCl, 10 mM succinate, 0.1 mM EGTA, and 10 mM HEPES, pH 7.4. Homogenates were then centrifuged at 700*g* 4 °C for 10 min. Supernatants were recovered and further centrifuged at 10,000*g* for 15 min. The resulting pellet (crude mitochondria) was resuspended in 1 ml, layered onto 8 ml of 30% Percoll (v:v) and centrifuged at 95,000*g* for 30 min. The closest layer to the tube bottom belonging to mitochondria was rinsed twice by centrifuging at 10,000*g* for 15 min and stored until use. Mitochondria from SH-SY5Y cells were isolated by digitonin fractionation as described previously [36].

2.6. Western blotting

Cells or mouse brains were lysed in lysis buffer (20 mM Tris-Cl, pH 7.4, 0.5% Triton X-100, 10% sucrose, 1 mg/ml aprotinin, and 10 mM phenylmethane sulfonyl fluoride) for 30 min at 4° and centrifuged at 16,000*g* for 15 min. Samples (25–50 μg of protein/lane) were resolved by SDS-PAGE (Bio-Rad, 3450124) and transferred to nitrocellulose membranes (Bio-Rad, 1704271). Blots were probed with the antibodies listed in Table 1. After overnight incubation at 4 °C, bound antibodies were visualized using horseradish peroxidase-coupled secondary antibodies and the Amersham™ Prime Western Blotting Detection Reagent (GE Healthcare; 32106).

2.7. Selfie RT-qPCR

Selfie qRT-PCR was performed as described in Podlesniy and Trullas [37]. Briefly, brain homogenates were prepared and diluted in 100ST buffer (DireCtquant). Then, 2.5 mM IDE reverse primer (5′-actgtgaaaagccgagaga-3′) was annealed with samples at 70 °C for 5 min. Samples were incubated with RiboLock RNase Inhibitor (ThermoFisher Sci., EO0381) and glycerol or Maxima H Minus Reverse Transcriptase (ThermoFisher Sci., EP0751), and retrotranscribed for 30 min at 60 °C and 5 min at 85 °C. Finally, 2.5 mM IDE forward primer (5′- actgtgaaagccgagaga -3′) was added and amplified by conventional RT-qPCR (5 min at 95 °C, followed by 40 cycles of 15 s at 95 °C, 35 s at 60 °C and 25 s at 72 °C), using iTaq™ Universal SYBR® Green Supermix (Bio-Rad). mRNA expression was calculated as difference in expression of the sample containing reverse transcriptase minus sample containing glycerol.

2.8. Immunoprecipitation

Immunoprecipitation was performed using Dynabeads™ Protein G beads (Thermo Fisher Sci., 10003D). Mouse *anti*-IDE monoclonal antibody (2 μg; Santa Cruz Biotech., sc-393887) or goat *anti*-NEP polyclonal antibody (2 μg; R&D Systems, AF1126) were incubated with beads (1.5 mg) for 40 min in rotation. Then, brain homogenates (1 mg) were incubated with bead-antibody complexes for 1 h at room temperature. The immunoprecipitated proteins were eluted by adding 50 mM glycine pH 2.8 and then analyzed by western blotting.

2.9. Cholesterol and mGSH quantification

50 μg of brain homogenates or 0.05×10^6 cells were mixed with a chloroform:isoporpanol:IGEPAL CA-630 (7:11:0.1) mixture and centrifuged at 13,000*g* for 10 min. Organic phase was recovered, transferred to another eppendorf and vacuum centrifuged for 30 min to remove remaining chloroform and organic solvent. The pellet was resuspended in 1x reaction buffer from the Amplex Red Cholesterol Assay kit (Thermo Fisher Sci., A12216) and analyzed following the guidelines provided by the supplier. Mitochondrial mGSH content was analyzed using the Glutathione Assay Kit (Sigma-Aldrich, CS0260-1 KT) according to the manufacturer's instructions. Samples were assayed after precipitation with 10% TCA.

2.10. IDE and NEP activity

10 μg of cell or brain lysates were mixed with 10 μM of the fluorogenic peptide Mca-RPPGFSAFK(Dnp)-OH (R&D Systems) in reaction buffer (100 mM Tris-Cl, pH 7.5, 50 mM NaCl, and 10 mM $ZnCl_2$) and the fluorescent intensity of the cleaved fragments was monitored during 30 min at 37 °C with excitation at 320 nm and emission at 405 nm. Insulin (10 μM, Thermo Fisher Sci., RP-10908), a competitive substrate of IDE or thiorphan (40 μM, Santa Cruz Biotech., sc-201287), a potent inhibitor of NEP, was added to distinguish the specific enzyme activities. In both cases, we first determined the dose that achieves maximum substrate cleavage inhibition using 10 μg of lysate (Supplementary Fig. S1). IDE activity was defined as the activity sensitive to insulin inhibition and NEP activity was defined as the activity sensitive to thiorphan inhibition.

2.11. Aβ degradation assay

Degradation of Aβ was measured by the incubation of 1 μM monomeric human Aβ1-42 in 1 ml of conditioned media from SH-SY5Y cells exposed to the indicated treatment. After 12 h of incubation at 37 °C, proteins were precipitated with TCA following the procedure described above and subjected to immunoblotting analysis.

2.12. Isolation of extracellular vesicles

Extracellular vesicles (EVs) were isolated from 4 days conditioned medium supplemented with 10% of exosome-depleted FBS by ultracentrifugation (100,000 g for 16 h). The medium was first centrifuged at 300*g* for 10 min followed by two centrifugations at 3,000*g* and 10,000*g* for 10 min and one last ultracentrifugation at 100,000*g* for 70 min to pellet the EVs. Pellets were rinsed in PBS and centrifuged again at 100,000*g* for 70 min. Finally, EVs were resuspended in lysis buffer, incubated at 4 °C for 30 min and then were centrifuged at 16,000*g* for 15 min. Supernatants were stored at −20 °C until use.

2.13. Statistics

All results are expressed as mean ± SD. Statistical significance was examined using the unpaired, two-tailed Student's *t*-test. A value of

Table 1
Details of the primary antibodies used in the current study.

Antibody	Company	Cat. No.	dilution
ACTB/actin	Sigma-Aldrich	A3853	1:30,000
Aβ(6E10)	Biolegend	803001	1:1,000
FLOT1	Santa Cruz Biotech.	sc-25506	1:200
4-HNE (IDE/4-HNE coIP)	Novus Biologicals	NB100-63093	1:1,000
4-HNE (NEP/4-HNE coIP)	R&D Systems	MAB3249	1:1,000
IDE	Merck Millipore	PC730	1:1,000
LC3B	Cell Signaling	2775S	1:1,000
NEP (human)	Merck Millipore	AB5458	1:500
NEP (mouse)	R&D Systems	AF1126	1:1,000
SQSTM1/P62	Abcam	Ab91526	1:1,000
TSG101	BD Bioscience	612696	1:1,000

$P < 0.05$ was considered statistically significant.

3. Results

3.1. Impaired function of IDE and NEP in APP-PSEN1-SREBF2 mice

We first determined the proteolytic activity of IDE and NEP in brain homogenates of 8-month-old wild-type (WT) and APP-PSEN1 mice with and without SREBF2 overexpression. We observed that the activity of both enzymes was significantly reduced in APP-PSEN1-SREBF2 mice compared to WT mice (Fig. 1A). The analysis of IDE and NEP protein levels in brain homogenates performed by immunoblotting reveled that IDE was increased in APP-PSEN1-SREBF2 mice while NEP levels remained unaltered regardless of genotype (Fig. 1B). qRT-PCR analysis also showed unchanged expression levels of *Nep* mRNA accompanied with an increase in *Ide* mRNA levels in the triple transgenic mice (Fig. 1C), indicating that the rise of IDE protein levels in these mice was due to an upregulated transcription, and it most likely reflects an adaptive response to IDE functional impairment.

3.2. In vivo treatment with 2-hydroxypropyl-β-cyclodextrin counteracts IDE changes and reduces Aβ brain content displayed by APP-PSEN1-SREBF2 mice

Previous data from cells and mice overexpressing mutant *App* transgenes showed that the administration of the cholesterol-lowering compound 2-hydroxypropyl-β-cyclodextrin (HP-β-CD) exerted a neuroprotective effect, lowering TAU and Aβ burden [38,39]. In mice, cognitive improvement after chronic HP-β-CD therapy was linked to diminished Aβ plaques, suggesting that the effect of the drug may be in part mediated by an enhanced clearance of Aβ [38,39]. We analyzed the effect of HP-β-CD administration (4 g/kg/day) in APP-PSEN1-SREBF2 mice. As expected, a significant decrease of cholesterol content was observed after treatment in both total homogenate and isolated mitochondria from mice that overexpress SREBF2 compared to WT mice (Fig. 2A). Normalization of mitochondrial cholesterol levels in treated mice resulted in the recovery of mGSH content (Fig. 2B). The egress of brain cholesterol by HP-β-CD was not sufficient to significantly recover NEP activity in the triple transgenic mice (Fig. 2C). No changes were observed regarding NEP protein levels after HP-β-CD administration (Fig. 2D). In contrast, the cholesterol-lowering agent prevented the increased expression of IDE observed in brain extracts from APP-PSEN1-SREBF2 mice (Fig. 2D) and significantly raised its proteolytic activity (Fig. 2C). Interestingly, the increase of IDE activity after HP-β-CD treatment was accompanied with a lower accumulation of Aβ in brain extracts (Fig. 2E).

3.3. Increased levels of oxidatively-modified IDE and NEP in brains from APP-PSEN1-SREBF2 mice and protective effect of 2-hydroxypropyl-β-cyclodextrin treatment

Evidence indicates that IDE and NEP are oxidatively impaired in AD [17,18]. Both peptidases have been described to react with the lipid peroxidation product 4-hydroxynonenal (4-HNE), with the concomitant formation of inactive protein adducts [40,41]. Moreover, Aβ incubation in SH-SY5Y cells has been shown to increase the presence of 4-HNE-NEP and 4-HNE-IDE adducts [41,42]. To analyze whether IDE and NEP are modified by oxidative damage in brain extracts from APP-PSEN1-SREBF2 mice, 4-HNE-adducted and unmodified levels of both AβDPs were determined by immunoprecipitation followed by Western blot analysis with the corresponding antibody. As shown, the ratio of 4-HNE-IDE adducts to total IDE was 1.8 times higher in APP-PSEN1-SREBF2 brain compared to WT brain (Fig. 3A). After HP-β-CD administration the 4-HNE-IDE/IDE ratio in extracts of WT and triple

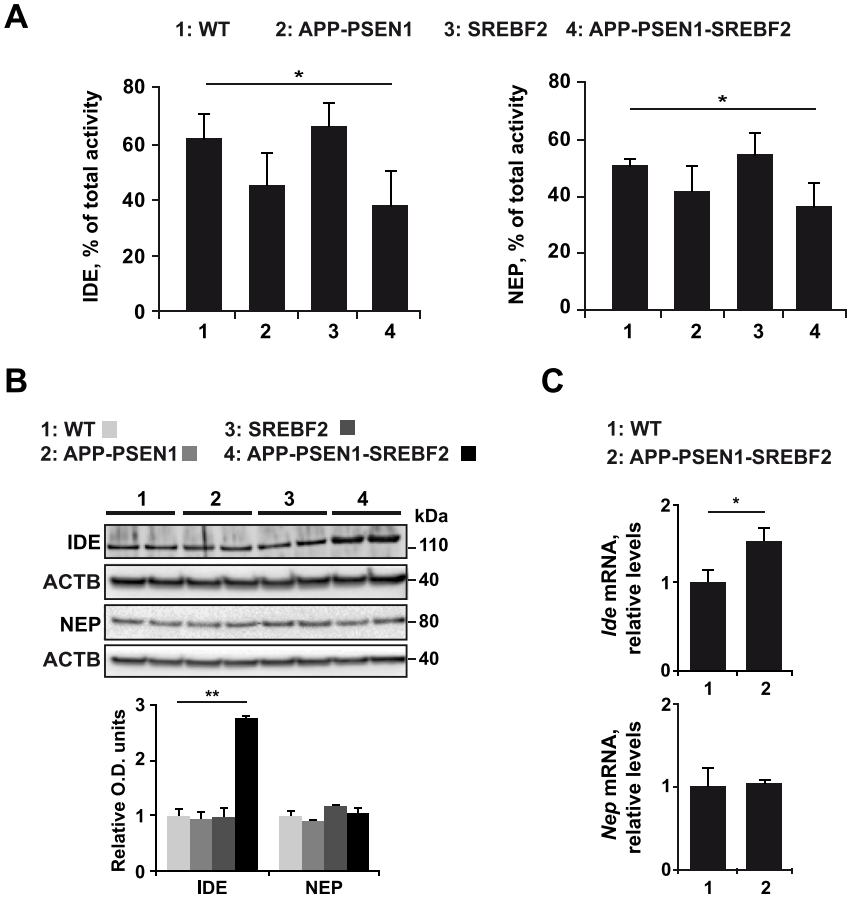

Fig. 1. Impaired IDE and NEP enzymatic activities in APP-PSEN1-SREBF2 mice. **A**) IDE and NEP activities assessed in brain homogenates of 7-mo-old WT and the indicated transgenic mice using a fluorogenic peptide substrate. The specific activities of both IDE and NEP enzymes were calculated by subtracting residual fluorescent intensity after incubation with the inhibitors insulin and thiorphan, respectively, and were expressed as percentage of total endopeptidase activity. **B**) Representative immunoblot of IDE and NEP. Protein expression was normalized to β-actin (ACTB) intensity and expressed as relative optical density (O.D.) units. **C**) *Ide* and *Nep* mRNA expression analyzed by Selfie qRT-PCR. mRNA values were normalized to total DNA expression and reported as relative levels referred to the expression in WT mice. Significant differences were expressed as * $p \leq 0.05$; ** $p \leq 0.01$.

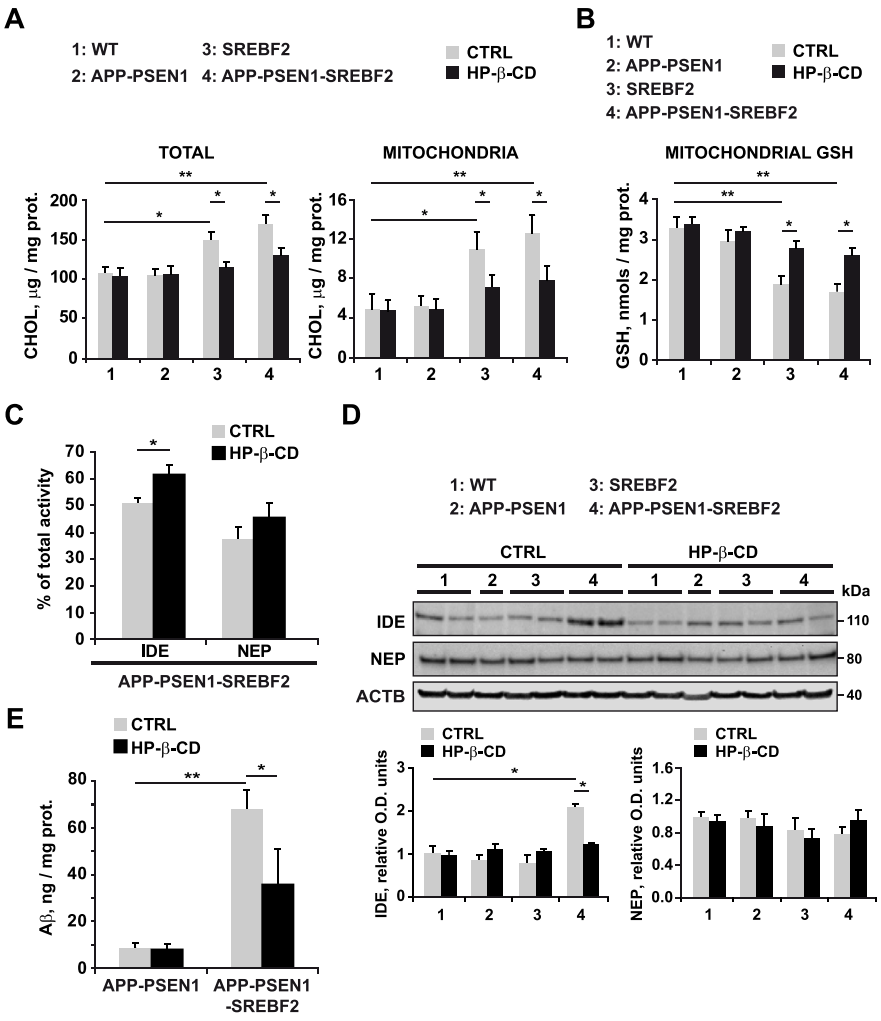

Fig. 2. *In vivo* treatment with 2-hydroxypropyl-β-cyclodextrin (HP-β-CD) recovers IDE activity and expression in APP-PSEN1-SREBF2 mice. 7-mo-old WT and the indicated transgenic mice were treated with 4 g/kg HP-β-CD twice a week for 10 weeks. Saline solution was used as control. A) Total and mitochondrial cholesterol levels in brain homogenates. B) mitochondrial GSH levels in brain homogenates. C) IDE and NEP enzymatic activities assessed using a fluorogenic peptide substrate. The specific activities of both IDE and NEP enzymes were calculated by subtracting residual fluorescent intensity after incubation with the inhibitors insulin and thiorphan, respectively, and were expressed as percentage of total endopeptidase activity. D) Representative immunoblot of IDE and NEP. Densitometric values of specific protein bands were normalized to β-actin (ACTB) intensity and expressed as relative optical density (O.D.) units. E) Brain were homogenized with guanidine HCl extraction buffer and the homogenates were analyzed by ELISAs for quantitative assessment of the human Aβ(1–42) content. Significant differences between conditions were expressed as * $p \leq 0.05$; ** $p \leq 0.01$.

transgenic brains was reduced below values of untreated WT mice (Fig. 3A). Brain extracts from APP-PSEN1-SREBF2 mice also showed an increased 4-HNE-NEP/NEP ratio compared to samples from APP-PSEN1 mice, which displayed almost unnoticeable presence of 4-HNE-NEP adducts (Fig. 3B). The content of oxidatively-modified NEP in the triple transgenic mice was reduced by 35% after HP-β-CD treatment (Fig. 3C).

3.4. Cholesterol-mediated mGSH depletion promotes the impairment of IDE and NEP proteolytic activities induced by Aβ

Mitochondria have emerged as major contributors of Aβ-induced oxidative stress. Aβ progressively accumulates in mitochondria of AD brain [43–45], and the interaction of Aβ with mitochondria can result in mitochondrial dysfunction and ROS generation [43,45–47], provided that the mitochondrial antioxidant defense system is impaired [33,48]. Having previously shown that Aβ-induced oxidative stress is enhanced by mGSH depletion [32–34], we analyzed the contribution of the cholesterol-mediated mGSH depletion in the Aβ-induced oxidative impairment of AβDPs. SH-SY5Y cells were incubated with a water-soluble cholesterol complex (CHO:MCD, cholesterol:methyl-β-cyclodextrin) and exposed to oligomeric Aβ. The increase of intracellular cholesterol content after treatment was confirmed by staining with filipin, a fluorescent polyene antibiotic that specifically binds cholesterol, and that showed a higher and homogeneous intracellular staining in CHO:MCD-treated cells (Fig. 4A). Quantitation of total cholesterol levels was also assessed by a fluorometric assay (Fig. 4B), and as expected, the increase of sterol levels in CHO:MCD-treated cells was accompanied with a significant depletion of mGSH content compared to

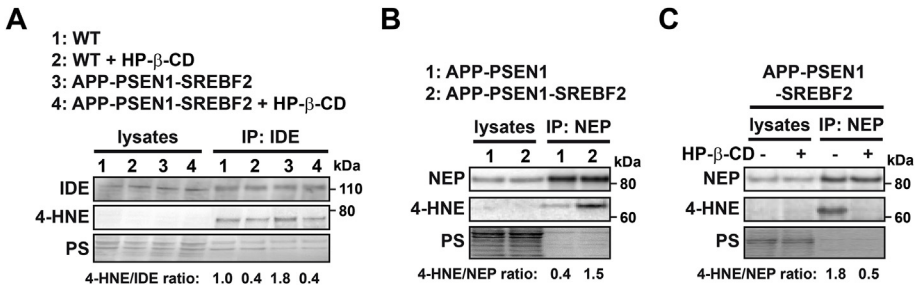

Fig. 3. High levels of oxidized IDE and NEP in APP-PSEN1-SREBF2 mice reverted after *in vivo* treatment with 2-hydroxypropyl-β-cyclodextrin (HP-β-CD). 7-mo-old WT and the indicated transgenic mice received HP-β-CD (4 g/kg) twice a week for 10 weeks or saline solution as control. A) Brain lysates were first immunoprecipitated with an *anti*-IDE antibody and then analyzed by immunoblotting for IDE and its oxidized adduct using an *anti*-HNE antibody. B) and C) Brain lysates were first immunoprecipitated with an *anti*-NEP antibody and then analyzed by immunoblotting for NEP and its oxidized adduct using an *anti*-HNE antibody. The relative ratio of the oxidized over total enzyme was determined by dividing the intensity levels of the 4-HNE blot with the levels of the corresponding IDE or NEP blot after normalized to the total amount of protein stained with Ponceau S (PS).

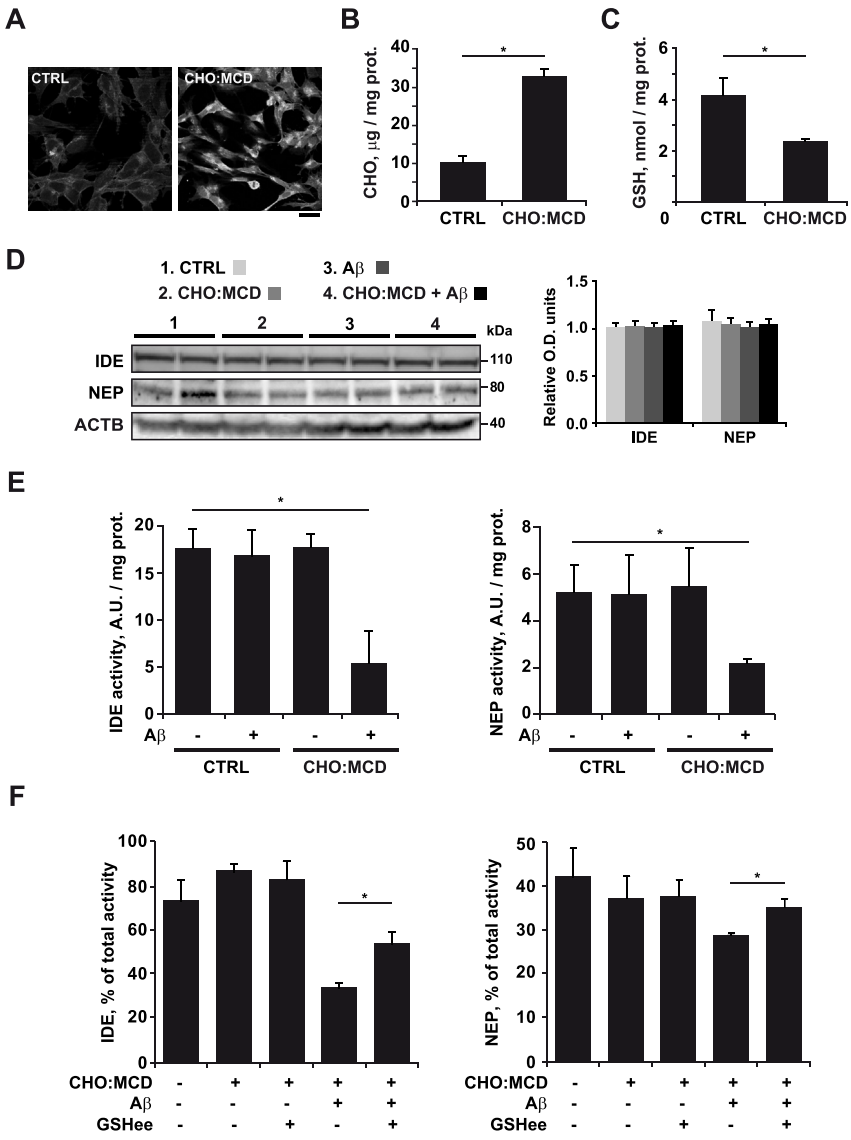

Fig. 4. Impairment of IDE and NEP activities in cholesterol-enriched SH-SY5Y cells after Aβ exposure, which is prevented by GSH ethyl ester treatment. SH-SY5Y cells were treated with the cholesterol:methylcyclodextrin (CHO:MCD) complex (50 µg/mL) for 1 h. A) Filipin staining of free cholesterol. Representative images showing enhanced fluorescence in CHO:MCD-treated cells. B) Total cholesterol and C) mitochondrial GSH (mGSH) levels of cellular extracts o control (CTRL) and CHO:MCD-treated cells. D) Representative immunoblots of IDE and NEP. Densitometric values of specific protein bands were normalized to β-actin (ACTB) intensity and expressed as relative optical density (O.D.) units. E) Activity of IDE and NEP in cellular lysates from control (CTRL) and CHO:MCD-treated cells with and without Aβ (5 µM) exposure for 24 h. The specific activities of both IDE and NEP enzymes were calculated by subtracting residual fluorescent intensity of the cleaved fluorogenic substrate, after incubation with the inhibitors insulin and thiorphan, respectively (A.U.: arbitrary units). F) Effect of GSH ethyl ester (GSHee, 4 mM) treatment on IDE and NEP activities analyzed in cellular lysates of control (CTRL) and CHO:MCD-treated cells exposed to Aβ (5 µM) for 24 h. IDE and NEP activity is expressed as percentage of total endopeptidase activity. Significant differences were expressed as * $p \leq 0.05$.

untreated cells (Fig. 4C). After cholesterol enrichment, cells were incubated with Aβ (5 µM) for 24 h and expression levels and activity of IDE and NEP were assessed. As shown, CHO:MCD treatment did not modify the cellular content of IDE and NEP, regardless of Aβ incubation (Fig. 4D). However, the proteolytic activity of both enzymes was significantly affected in cholesterol-enriched cells exposed to Aβ (Fig. 4E). Remarkably, preincubation with GSH ethyl ester (GSHee), a membrane-permeable GSH form that restores the depleted pool of mGSH in cholesterol-enriched cells (data not shown) [49] prevented Aβ-induced inhibition of IDE and NEP activities in CHO:MCD-treated cells (Fig. 4F). Thus, these findings indicate that the enhanced susceptibility to Aβ displayed by both peptidases in cholesterol-enriched cells is largely due to mGSH depletion.

3.5. Cellular cholesterol enrichment enhances IDE release by stimulating secretory autophagy

It has been described that IDE can be released to the extracellular space by an unconventional secretory pathway that presumably involves exosomes formation [14,15]. Given that extracellular vesicles (EVs), including exosomes, are enriched in cholesterol and their cellular release has been reported to be cholesterol-dependent [50], we next evaluated whether changes in cholesterol levels can affect IDE secretion. SH-SY5Y cells were cholesterol-enriched with the CHO:MCD complex and the EVs were isolated from cell-free conditioned media by ultracentrifugation. Samples from CHO:MCD-treated cells showed increased content of EV marker proteins such as tumor susceptibility gene 101 (TGS101) and flotillin 1 (FLOT1), indicative of greater EV release (Fig. 5A). IDE presence was only observed in EV from cholesterol-enriched cells (Fig. 5A) and was associated with an increased enzymatic activity (Fig. 5B). In contrast, control cells displayed almost neglectable extracellular IDE activity (Fig. 5B). In astrocytes, IDE secretion has been associated with an autophagy-based secretory pathway [16]. Autophagy can also influence Aβ release to the extracellular space and thereby affect Aβ plaque burden [51]. Moreover, we have recently demonstrated that high cholesterol levels not only prevents Aβ degradation but also stimulates unconventional secretion of Aβ through altering the autophagy flux [49]. To test whether the enhanced release of IDE in cholesterol-enriched cells is autophagy-dependent, cells were incubated with wortmannin, a selective and irreversible PI3-kinase inhibitor that blocks autophagosome formation. We first analyzed the levels of lipidated microtubule-associated protein 1 light chain 3 B (MAP1LC3B/LC3B), a marker of autophagosome formation, and the levels of the autophagy substrate sequestosome 1 (SQSTM1/p62). As shown, the cellular cholesterol-enrichment stimulated autophagosome formation, with presence of lipidated LC3B (LC3B-II) (Fig. 5C).

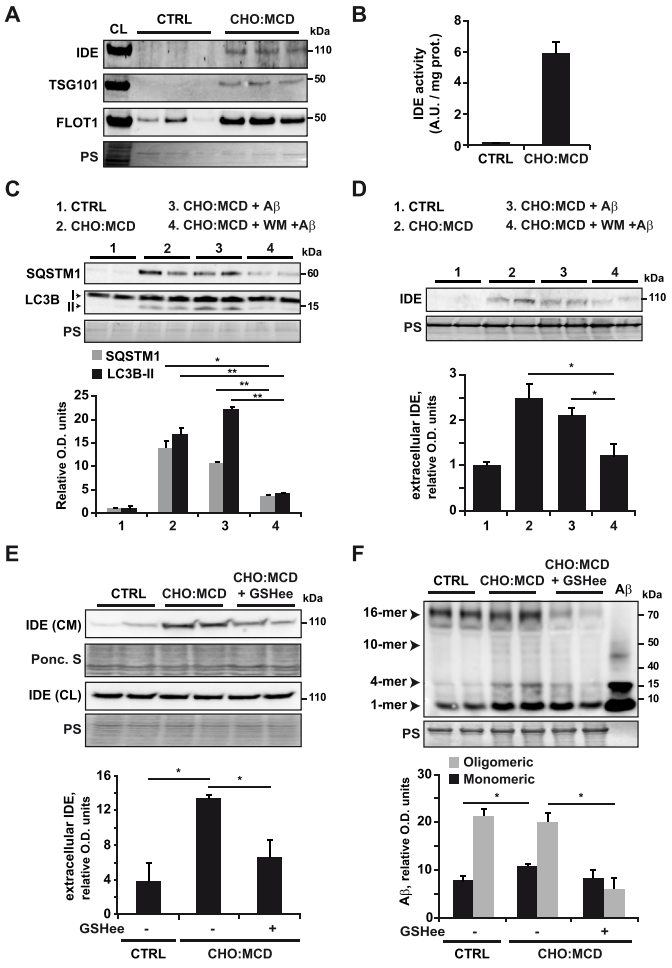

Fig. 5. Cholesterol enrichment in SH-SY5Y cells enhances the release of inactive IDE through secretory autophagy and downregulates the extracellular Aβ-degrading activity. SH-SY5Y cells were treated with the cholesterol:methylcyclodextrin (CHO:MCD) complex (50 μg/mL) for 1 h. EVs were recovered by differential centrifugation of cell-free conditioned media collected after 96 h of culture. A) Representative immunoblots of IDE and the vesicular markers TSG101 and flotillin-1. Ponceau S (PS) staining was used as total protein marker. (CL: cellular lysate). B) IDE activity in EVs. The specific activity of IDE was calculated by subtracting residual fluorescent intensity of the cleaved fluorogenic substrate, after incubation with the inhibitors insulin (A.U.: arbitrary units). C) and D) CHO:MCD-treated cells were incubated with the autophagy inhibitor wortmannin (WM, 5 μM) and Aβ (5 μM) for 24 h. C) Representative immunoblots for SQSTM1 and LC3B protein levels in whole-cell lysates. D) Representative immunoblots for IDE levels analyzed in 48 h conditioned media. Densitometric values of specific protein bands were normalized to Ponceau S (PS) intensity and expressed as relative optical density (O.D.) units. E) and F) CHO:MCD-treated cells were incubated with GSH ethyl ester (GSHee, 4 mM) for 48 h and cell media (CM) and lysates (CL) were collected. E) Representative western blots of IDE protein levels analyzed in CM and CL. Extracellular IDE expression was normalized to Ponceau S (PS) and expressed as relative optical density (O.D.) units. F) Representative Western blot of Aβ levels analyzed in CM. 48 h conditioned media were incubated with 1 μM monomeric Aβ for 12 h and after protein precipitation by TCA the remaining monomeric Aβ and its aggregation in oligomers was assessed by immunoblot. Densitometric values of monomeric bands (1-mer) and oligomeric bands (4- to 16-mer) were normalized to Ponceau S (PS) intensity and expressed as relative optical density (O.D.) units. Significant differences between conditions were expressed as * $p \leq 0.05$.

Lipidated LC3B levels further increased in cholesterol-enriched cells exposed to Aβ (Fig. 5C). Also, in agreement of what we had previously described [49], the levels of SQSTM1/p62 rose in cholesterol-enriched cells (Fig. 5C), indicative of an autophagy flux blockage by cholesterol. Wortmaninn exposure prevented both autophagosome formation and SQSTM1/p62 accumulation (Fig. 5C) and significantly reduced the enhanced extracellular release of IDE induced by cholesterol in cells exposed to Aβ (Fig. 5D), indicating that cholesterol can regulate IDE secretion by modulating autophagy flux. Our previous studies showed that autophagy induction in cholesterol-enriched cells was due to an exacerbated Aβ-induced oxidative stress, and GSHee administration significantly inhibited both autophagosome formation and secretory autophagy by reducing the mitochondrial oxidative stress [49]. Hence, as expected the recovery of mitochondrial GSH in CHO:MCD-treated cells after GSHee incubation significantly reduced IDE release (Fig. 5E) without affecting intracellular IDE levels (Fig. 5E).

3.6. Conditioned media from cholesterol-enriched cells show low Aβ-degrading activity

Having established a link between high cholesterol levels and impaired IDE and NEP enzymatic activity, we next analyzed whether cellular cholesterol content can regulate extracellular Aβ degradation. Conditioned media from control and cholesterol-enriched cells were incubated with 1 μM monomeric Aβ for 12 h. After the incubation period, the remaining levels of Aβ were analyzed by Western blot. As shown, despite the enhanced release of IDE displayed by cholesterol-enriched cells, samples from CHO:MCD-treated cells showed increased monomeric Aβ levels compared to control cells (Fig. 5F), which resulted in increased formation of Aβ oligomers (Fig. 5F). Remarkably, the low Aβ-degrading activity observed after cholesterol enrichment was reverted by GSHee treatment (Fig. 5F). The recovery of mGSH in CHO:MCD-treated cells significantly prevented the appearance of the most toxic oligomeric forms of Aβ (Fig. 5F). Overall these findings highlight the key role of mitochondrial oxidative stress in regulating the proteolytic clearance of Aβ and pointing to GSHee as a helpful tool in maintaining a proper activity of Aβ-degrading enzymes.

4. Discussion

In the present study, using AD mouse models with a high brain cholesterol burden and cholesterol-enriched neuroblastoma cells, we have shown that functionality of the main Aβ-degrading enzymes is regulated by cholesterol-enhanced oxidative damage. Remarkably, decreased IDE and NEP activities are not observed in SREBF2 mice, neither in cholesterol-enriched cells, unless they are exposed to Aβ; hence, cholesterol is needed but is not sufficient to promote the oxidative impairment of both enzymes, which requires Aβ presence. Aβ toxicity linked to mitochondrial dysfunction has been described to mediate or even initiate key pathologic molecular cascades in AD [52]. Aβ interact with mitochondria inducing ROS [46,53], and high cholesterol levels can enhance this Aβ-induced oxidative stress and damage through depleting the mGSH content [32,33]. Our previous studies also showed that treatment with GSHee, which recovers the cholesterol-depleted mGSH levels, significantly prevented the main pathological hallmarks of AD in APP-PSEN1-SREBF2 mice, including Aβ deposition [34]. Here, we further demonstrate that the administration of this soluble form of GSH can counteract the alterations in IDE and NEP function due to cholesterol rise. Interestingly, its protective effect was not limited to intracellular AβDPs; the incubation with GSHee also resulted in improved degradation of extracellular Aβ with lower formation of Aβ oligomeric species.

We have observed that while NEP expression remains unaltered, the decrease in IDE activity is associated with upregulated protein and mRNA levels in APP-PSEN1-SREBF2 mice. This rise of IDE expression may be part of a compensatory response, although insufficient to counteract the impaired activity. A similar outcome has been reported in vessels from patients with cerebral amyloid angiopathy showing overexpression of IDE associated to low enzymatic activity [54]. Apart from that, several reports display mixed results regarding changes in

the expression of both peptidases. For instance, an age-dependent decline in the expression of both IDE and NEP has been reported in neuronal cells and in AD vulnerable brain areas, such as cortex and hippocampus [17–19,25]. In contrast, NEP has been found upregulated in reactive astrocytes surrounding amyloid plaques in AD mice [55]. Interestingly, in line with our results, hippocampus from high-cholesterol-fed C57BL/6 mice displays high IDE expression, without changes in NEP protein levels [56]. A link between cholesterol and NEP expression has also been described in studies using SH-SY5Y cells stably overexpressing APP_{695} [57]. Belyaev et al. show that NEP expression is transcriptionally regulated by the APP intracellular domain (AICD), and reduction of membrane cholesterol levels by methyl-β-cyclodextrin significantly affects NEP expression by lowering AICD levels, presumably synthesized through a cholesterol-dependent endocytic pathway. Unlike this study, we have not observed any significant change in NEP levels after the *in vivo* treatment with HP-β-CD, possibly because the reduction of cholesterol levels (with values above WT levels) is not strong enough to affect the endocytic pathway. Cholesterol has also been reported to regulate the localization of mature NEP to lipid rafts, where the substrate Aβ accumulates, nonetheless, the location does not seem to modulate its protease activity [58]. Beside changes in the expression and location, activity of AβDPs can be regulated by post-translational modifications. Both IDE and NEP are inactivated by oxidation [40]. Oxidative products (4-HNE adducts of IDE and NEP), similar to those displayed by APP-PSEN1-SREBF2 mice, have been found in brain extracts from AD patients [17–19]. Furthermore, depositions of both IDE and NEP have been reported in senile plaques, particularly in brains from sporadic late-onset AD patients [23], and although the mechanisms involved are unknown, it is likely that an enhanced and sustained oxidative stress may promote the conformational changes needed to convert the enzymes from “natively folded-active” to “aggregated-inactive” forms. Recent studies have also reported that oxidative stress can compromise IDE function indirectly by inducing phospholipase A2 group 3 (Pla2g3) expression which in turn downregulates IDE expression [59].

We have showed that the oxidatively-modified forms of IDE and NEP decrease in the triple transgenic mice after treatment with the cholesterol-sequestering agent HP-β-CD. The reduction of HNE-adducts of IDE is accompanied with a significant recovery of its activity. Intriguingly, the increased IDE activity is observed despite that protein levels are lowered to control values after HP-β-CD treatment, which further reinforces the notion that cholesterol exerts a post-translational control of IDE activity independently of its levels, whereas the transcriptional regulation of IDE would be more likely linked to changes of enzyme functionality. In contrast, the reduction of NEP oxidative damage in APP-PSEN1-SREBF2 mice after cholesterol egress does not recover its activity, suggesting that at least *in vivo* other cholesterol-independent mechanisms may play a role.

Cholesterol enrichment results in increased release of IDE through an unconventional secretory pathway that involves EVs. Of note, a certain enzymatic activity is detected associated to the presence of IDE protein in EVs, although to the same extent that the intracellular IDE activity displayed by cholesterol-enriched cells exposed to Aβ, which is significantly low compared to untreated cells. Neither IDE presence nor endopeptidase activity is observed in EVs isolated from untreated control cells, in agreement with a recent article that questions the release of IDE in cultured cells [60]. Moreover, and unlike cholesterol-mediated alterations of IDE function, the release of IDE through EVs after cellular cholesterol enrichment does not require Aβ exposure. Growing evidence indicate that cholesterol contributes to EVs biogenesis and release [50]. Cellular cholesterol loading, directly or by treatment with U18666A, which mimics the cellular phenotype of the cholesterol-related Niemann-Pick disease, stimulates EV release [61,62]. Also, enhanced release of cholesterol-rich EVs has been observed after overexpression of the cholesterol transporter ABCA1, further confirming the link between cholesterol metabolism and EVs [63]. EVs fall in two categories according to their subcellular origin and size, microvesicles (100 nm–1 μm) budded directly from the plasma membrane, and exosomes (50–100 nm) that arise from endosome-derived multivesicular bodies [64]. We have not specifically assessed by which type of vesicle is IDE secreted after cellular cholesterol enrichment, further analyses using electron microscopy would be required to determine the vesicle size and type; despite that, previous studies point to the involvement of exosomes in IDE secretion [14,15], in collaboration with the autophagy pathway [16]. Interestingly, recent studies suggest a high crosstalk between exosomes biogenesis and autophagy, with shared molecular machinery. In neuronal cells, both autophagic degradation and exosome secretion are used to eliminate protein aggregates, and when autophagy or lysosomes are impaired, exosome release is enhanced [65]. Recently, we showed in APP-PSEN1-SREBF2 mice that cholesterol promotes this autophagy-dependent secretory pathway, by blocking the Aβ-induced autophagy flux while autophagosomes formation is stimulated [49]. Now, using the autophagy inhibitor wortmannin we have found lower levels of extracellular IDE in media from cholesterol-enriched cells after autophagy inhibition, supporting the notion that cholesterol-induced release of IDE is under the control of this unconventional autophagy-based secretory pathway.

Conditioned media from cholesterol-enriched cells show reduced capacity of Aβ degradation associated with an increased formation of the most toxic oligomeric assemblies [66], and both alterations are counteracted by GSHee incubation. Our findings point to improved IDE activity as the responsible for the enhanced degradation of extracellular Aβ after GSHee treatment, although the involvement of other proteases cannot be excluded. For instance, plasmin, a serine protease present in the extracellular matrix, can degrade Aβ aggregates [67]. However, plasminogen deficiency in mice does not result in increased brain or plasma Aβ levels [68], unlike IDE and NEP knockout mice that show increased deposition of Aβ [69,70]. The relevance of NEP and IDE in Aβ metabolism has been widely proved in AD mice [71,72] and therapeutic interventions based on increasing their expression have been proposed. Our studies show that IDE and NEP are highly sensitive to the enhanced oxidative stress promoted by high cholesterol levels, thus, strategies aimed to prevent the oxidative inactivation of both enzymes could improve Aβ clearance while avoiding potential side effects concomitant to enzyme expression manipulation. Under stressful conditions, cells can activate a stress response consisting of a pro-survival network controlled by several genes termed vitagenes [73]. The activation of the vitagene system, with up-regulation of antioxidant molecules such as heme oxigenases, thioredoxin, and the GSH and sirtuin systems, restores the cellular redox homoestasis and counteracts the deleterious effect of pro-oxidant insults [73]. Different pharmacological and/or nutritional approaches that potentiate these endogenous defense mechanisms have recently been demonstrated to be neuroprotective [74–76], most of them acting in a hormetic dose response [77]. Thus, given the relationship between oxidative stress and IDE/NEP proteolytic activites, the pharmacological stimulation of the vitagene system and its hormetic response could be explored as new avenues for therapeutic interventions.

In conclusion, our data reveal a novel mechanism connecting cholesterol-induced mitochondrial oxidative stress with reduced Aβ clearance and AD progression, and support antioxidant and cholesterol lowering compounds as protective therapies against NEP and IDE inactivation and Aβ accumulation.

Disclosure of interest

The authors declare that they have no competing interests.

Acknowledgement

The authors are grateful to Dr. R. Trullàs and Dr. G. Mengod, and their respective group members, for the helpful insights and technical

support. This work was supported by the Ministerio de Economía y Competitividad, Spain [SAF2013-47246-R and RTI2018-095572-B-100 to A.C., SAF2015-66515-R to A.M.]; the FEDER (Fondo Europeo de Desarrollo Regional, Unión Europea. “Una manera de hacer Europa”); the Fundació La Marató de TV3, Spain [2014-0930 to A.C.]; the Instituto de Salud Carlos III, Spain [PI16/00930 to M.M]; the Agencia de Gestió d’Ajuts Universitaris i de Recerca, Spain [2017_SGR_177]; and the CERCA Programme from the Generalitat de Catalunya, Spain. C.dD. has a FPU fellowship from Ministerio de Ciencia, Innovación y Universidades, Spain.

The graphical abstract was created with images adapted from Servier Medical Art templates, which are licensed under a Creative Commons Attribution 3.0 Unported License; https://smart.servier.com.

Appendix A. Supplementary data

Supplementary data to this article can be found online at https://doi.org/10.1016/j.redox.2019.101283.

References

[1] D.J. Selkoe, J. Hardy, The amyloid hypothesis of alzheimer's disease at 25 years, EMBO Mol. Med. 8 (6) (2016) 595–608.
[2] R.J. Bateman, L.Y. Munsell, J.C. Morris, R. Swarm, K.E. Yarasheski, D.M. Holtzman, Human amyloid-beta synthesis and clearance rates as measured in cerebrospinal fluid in vivo, Nat. Med. 12 (7) (2006) 856–861.
[3] K.G. Mawuenyega, W. Sigurdson, V. Ovod, L. Munsell, T. Kasten, J.C. Morris, K.E. Yarasheski, R.J. Bateman, Decreased clearance of cns beta-amyloid in alzheimer's disease, Science 330 (6012) (2010) 1774.
[4] J.M. Tarasoff-Conway, R.O. Carare, R.S. Osorio, L. Glodzik, T. Butler, E. Fieremans, L. Axel, H. Rusinek, C. Nicholson, B.V. Zlokovic, B. Frangione, et al., Clearance systems in the brain-implications for alzheimer disease, Nat. Rev. Neurol. 11 (8) (2015) 457–470.
[5] T. Saido, M.A. Leissring, Proteolytic degradation of amyloid beta-protein, Cold Spring Harb. Perspect. Med. 2 (6) (2012) a006379.
[6] H. Kanemitsu, T. Tomiyama, H. Mori, Human neprilysin is capable of degrading amyloid beta peptide not only in the monomeric form but also the pathological oligomeric form, Neurosci. Lett. 350 (2) (2003) 113–116.
[7] S. Fukami, K. Watanabe, N. Iwata, J. Haraoka, B. Lu, N.P. Gerard, C. Gerard, P. Fraser, D. Westaway, P. St George-Hyslop, T.C. Saido, Abeta-degrading endopeptidase, neprilysin, in mouse brain: synaptic and axonal localization inversely correlating with abeta pathology, Neurosci. Res. 43 (1) (2002) 39–56.
[8] L. Fisk, N.N. Nalivaeva, J.P. Boyle, C.S. Peers, A.J. Turner, Effects of hypoxia and oxidative stress on expression of neprilysin in human neuroblastoma cells and rat cortical neurones and astrocytes, Neurochem. Res. 32 (10) (2007) 1741–1748.
[9] S.E. Hickman, E.K. Allison, J. El Khoury, Microglial dysfunction and defective beta-amyloid clearance pathways in aging alzheimer's disease mice, J. Neurosci. 28 (33) (2008) 8354–8360.
[10] H.G. Bernstein, U. Lendeckel, A. Bukowska, S. Ansorge, T. Ernst, R. Stauch, K. Trubner, J. Steiner, H. Dobrowolny, B. Bogerts, Regional and cellular distribution patterns of insulin-degrading enzyme in the adult human brain and pituitary, J. Chem. Neuroanat. 35 (2) (2008) 216–224.
[11] K. Vekrellis, Z. Ye, W.Q. Qiu, D. Walsh, D. Hartley, V. Chesneau, M.R. Rosner, D.J. Selkoe, Neurons regulate extracellular levels of amyloid beta-protein via proteolysis by insulin-degrading enzyme, J. Neurosci. 20 (5) (2000) 1657–1665.
[12] W.Q. Qiu, D.M. Walsh, Z. Ye, K. Vekrellis, J. Zhang, M.B. Podlisny, M.R. Rosner, A. Safavi, L.B. Hersh, D.J. Selkoe, Insulin-degrading enzyme regulates extracellular levels of amyloid beta-protein by degradation, J. Biol. Chem. 273 (49) (1998) 32730–32738.
[13] J. Zhao, L. Li, M.A. Leissring, Insulin-degrading enzyme is exported via an unconventional protein secretion pathway, Mol. Neurodegener. 4 (4) (2009).
[14] A. Bulloj, M.C. Leal, H. Xu, E.M. Castano, L. Morelli, Insulin-degrading enzyme sorting in exosomes: a secretory pathway for a key brain amyloid-beta degrading protease, J. Alzheimer's Dis. 19 (1) (2010) 79–95.
[15] I.Y. Tamboli, E. Barth, L. Christian, M. Siepmann, S. Kumar, S. Singh, K. Tolksdorf, M.T. Heneka, D. Lutjohann, P. Wunderlich, J. Walter, Statins promote the degradation of extracellular amyloid {beta}-peptide by microglia via stimulation of exosome-associated insulin-degrading enzyme (ide) secretion, J. Biol. Chem. 285 (48) (2010) 37405–37414.
[16] S.M. Son, M.Y. Cha, H. Choi, S. Kang, M.S. Lee, S.A. Park, I. Mook-Jung, Insulin-degrading enzyme secretion from astrocytes is mediated by an autophagy-based unconventional secretory pathway in alzheimer disease, Autophagy 12 (5) (2016) 784–800.
[17] D.S. Wang, N. Iwata, E. Hama, T.C. Saido, D.W. Dickson, Oxidized neprilysin in aging and alzheimer's disease brains, Biochem. Biophys. Res. Commun. 310 (1) (2003) 236–241.
[18] A. Caccamo, S. Oddo, M.C. Sugarman, Y. Akbari, F.M. LaFerla, Age- and region-dependent alterations in abeta-degrading enzymes: implications for abeta-induced disorders, Neurobiol. Aging 26 (5) (2005) 645–654.
[19] R. Russo, R. Borghi, W. Markesbery, M. Tabaton, A. Piccini, Neprylisin decreases uniformly in alzheimer's disease and in normal aging, FEBS Lett. 579 (27) (2005) 6027–6030.
[20] K. Yasojima, H. Akiyama, E.G. McGeer, P.L. McGeer, Reduced neprilysin in high plaque areas of alzheimer brain: a possible relationship to deficient degradation of beta-amyloid peptide, Neurosci. Lett. 297 (2) (2001) 97–100.
[21] N.N. Nalivaevaa, L. Fisk, E.G. Kochkina, S.A. Plesneva, I.A. Zhuravin, E. Babusikova, D. Dobrota, A.J. Turner, Effect of hypoxia/ischemia and hypoxic preconditioning/reperfusion on expression of some amyloid-degrading enzymes, Ann. N. Y. Acad. Sci. 1035 (2004) 21–33.
[22] X. Zhang, W. Le, Pathological role of hypoxia in alzheimer's disease, Exp. Neurol. 223 (2) (2010) 299–303.
[23] V.B. Dorfman, L. Pasquini, M. Riudavets, J.J. Lopez-Costa, A. Villegas, J.C. Troncoso, F. Lopera, E.M. Castano, L. Morelli, Differential cerebral deposition of ide and nep in sporadic and familial alzheimer's disease, Neurobiol. Aging 31 (10) (2010) 1743–1757.
[24] J. Wang, K. Ohno-Matsui, I. Morita, Cholesterol enhances amyloid beta deposition in mouse retina by modulating the activities of abeta-regulating enzymes in retinal pigment epithelial cells, Biochem. Biophys. Res. Commun. 424 (4) (2012) 704–709.
[25] D.G. Cook, J.B. Leverenz, P.J. McMillan, J.J. Kulstad, S. Ericksen, R.A. Roth, G.D. Schellenberg, L.W. Jin, K.S. Kovacina, S. Craft, Reduced hippocampal insulin-degrading enzyme in late-onset alzheimer's disease is associated with the apolipoprotein e-epsilon 4 allele, Am. J. Pathol. 162 (1) (2003) 313–319.
[26] J.S. Miners, P. Kehoe, S. Love, Neprilysin protects against cerebral amyloid angiopathy and abeta-induced degeneration of cerebrovascular smooth muscle cells, Brain Pathol. 21 (5) (2011) 594–605.
[27] J. Kim, J.M. Basak, D.M. Holtzman, The role of apolipoprotein e in alzheimer's disease, Neuron 63 (3) (2009) 287–303.
[28] A.N. Lazar, C. Bich, M. Panchal, N. Desbenoit, V.W. Petit, D. Touboul, L. Dauphinot, C. Marquer, O. Laprevote, A. Brunelle, C. Duyckaerts, Time-of-flight secondary ion mass spectrometry (tof-sims) imaging reveals cholesterol overload in the cerebral cortex of alzheimer disease patients, Acta Neuropathol. 125 (1) (2013) 133–144.
[29] M. Heverin, N. Bogdanovic, D. Lutjohann, T. Bayer, I. Pikuleva, L. Bretillon, U. Diczfalusy, B. Winblad, I. Bjorkhem, Changes in the levels of cerebral and extracerebral sterols in the brain of patients with alzheimer's disease, J. Lipid Res. 45 (1) (2004) 186–193.
[30] R.G. Cutler, J. Kelly, K. Storie, W.A. Pedersen, A. Tammara, K. Hatanpaa, J.C. Troncoso, M.P. Mattson, Involvement of oxidative stress-induced abnormalities in ceramide and cholesterol metabolism in brain aging and alzheimer's disease, Proc. Natl. Acad. Sci. U.S.A. 101 (7) (2004) 2070–2075.
[31] J.H. Sun, J.T. Yu, L. Tan, The role of cholesterol metabolism in alzheimer's disease, Mol. Neurobiol. 51 (3) (2015) 947–965.
[32] J.C. Fernandez-Checa, A. Fernandez, A. Morales, M. Mari, C. Garcia-Ruiz, A. Colell, Oxidative stress and altered mitochondrial function in neurodegenerative diseases: lessons from mouse models, CNS Neurol. Disord. - Drug Targets 9 (4) (2010) 439–454.
[33] A. Fernandez, L. Llacuna, J.C. Fernandez-Checa, A. Colell, Mitochondrial cholesterol loading exacerbates amyloid beta peptide-induced inflammation and neurotoxicity, J. Neurosci. 29 (20) (2009) 6394–6405.
[34] E. Barbero-Camps, A. Fernandez, L. Martinez, J.C. Fernandez-Checa, A. Colell, App/ps1 mice overexpressing srebp-2 exhibit combined abeta accumulation and tau pathology underlying alzheimer's disease, Hum. Mol. Genet. 22 (17) (2013) 3460–3476.
[35] W. Yu, J.S. Gong, M. Ko, W.S. Garver, K. Yanagisawa, M. Michikawa, Altered cholesterol metabolism in niemann-pick type c1 mouse brains affects mitochondrial function, J. Biol. Chem. 280 (12) (2005) 11731–11739.
[36] J.C. Fernandez-Checa, M. Ookhtens, N. Kaplowitz, Effect of chronic ethanol feeding on rat hepatocytic glutathione. Compartmentation, efflux, and response to incubation with ethanol, J. Clin. Investig. 80 (1) (1987) 57–62.
[37] P. Podlesniy, R. Trullas, Absolute measurement of gene transcripts with selfie-digital pcr, Sci. Rep. 7 (1) (2017) 8328.
[38] M. Maulik, B. Ghoshal, J. Kim, Y. Wang, J. Yang, D. Westaway, S. Kar, Mutant human app exacerbates pathology in a mouse model of npc and its reversal by a beta-cyclodextrin, Hum. Mol. Genet. 21 (22) (2012) 4857–4875.
[39] J. Yao, D. Ho, N.Y. Calingasan, N.H. Pipalia, M.T. Lin, M.F. Beal, Neuroprotection by cyclodextrin in cell and mouse models of alzheimer disease, J. Exp. Med. 209 (13) (2012) 2501–2513.
[40] H. Shinall, E.S. Song, L.B. Hersh, Susceptibility of amyloid beta peptide degrading enzymes to oxidative damage: a potential alzheimer's disease spiral, Biochemistry (Mosc.) 44 (46) (2005) 15345–15350.
[41] R. Wang, S. Wang, J.S. Malter, D.S. Wang, Effects of hne-modification induced by abeta on neprilysin expression and activity in sh-sy5y cells, J. Neurochem. 108 (4) (2009) 1072–1082.
[42] R. Wang, S. Wang, J.S. Malter, D.S. Wang, Effects of 4-hydroxy-nonenal and amyloid-beta on expression and activity of endothelin converting enzyme and insulin degrading enzyme in sh-sy5y cells, J. Alzheimer's Dis. 17 (3) (2009) 489–501.
[43] M. Manczak, T.S. Anekonda, E. Henson, B.S. Park, J. Quinn, P.H. Reddy, Mitochondria are a direct site of a beta accumulation in alzheimer's disease neurons: implications for free radical generation and oxidative damage in disease progression, Hum. Mol. Genet. 15 (9) (2006) 1437–1449.
[44] C. Caspersen, N. Wang, J. Yao, A. Sosunov, X. Chen, J.W. Lustbader, H.W. Xu, D. Stern, G. McKhann, S.D. Yan, Mitochondrial abeta: a potential focal point for neuronal metabolic dysfunction in alzheimer's disease, FASEB J. 19 (14) (2005) 2040–2041.
[45] J.W. Lustbader, M. Cirilli, C. Lin, H.W. Xu, K. Takuma, N. Wang, C. Caspersen, X. Chen, S. Pollak, M. Chaney, F. Trinchese, et al., Abad directly links abeta to

mitochondrial toxicity in alzheimer's disease, Science 304 (5669) (2004) 448–452.
[46] C.S. Casley, L. Canevari, J.M. Land, J.B. Clark, M.A. Sharpe, Beta-amyloid inhibits integrated mitochondrial respiration and key enzyme activities, J. Neurochem. 80 (1) (2002) 91–100.
[47] S.M. Cardoso, I. Santana, R.H. Swerdlow, C.R. Oliveira, Mitochondria dysfunction of alzheimer's disease cybrids enhances abeta toxicity, J. Neurochem. 89 (6) (2004) 1417–1426.
[48] H. Hu, M. Li, Mitochondria-targeted antioxidant mitotempo protects mitochondrial function against amyloid beta toxicity in primary cultured mouse neurons, Biochem. Biophys. Res. Commun. 478 (1) (2016) 174–180.
[49] E. Barbero-Camps, V. Roca-Agujetas, I. Bartolessis, C. de Dios, J.C. Fernandez-Checa, M. Mari, A. Morales, T. Hartmann, A. Colell, Cholesterol impairs autophagy-mediated clearance of amyloid beta while promoting its secretion, Autophagy 14 (7) (2018) 1129–1154.
[50] F.W. Pfrieger, N. Vitale, Cholesterol and the journey of extracellular vesicles, J. Lipid Res. 59 (12) (2018) 2255–2261.
[51] P. Nilsson, K. Loganathan, M. Sekiguchi, Y. Matsuba, K. Hui, S. Tsubuki, M. Tanaka, N. Iwata, T. Saito, T.C. Saido, Abeta secretion and plaque formation depend on autophagy, Cell Rep. 5 (1) (2013) 61–69.
[52] R.H. Swerdlow, Mitochondria and mitochondrial cascades in alzheimer's disease, J. Alzheimer's Dis. 62 (3) (2018) 1403–1416.
[53] M. Manczak, T.S. Anekonda, E. Henson, B.S. Park, J. Quinn, P.H. Reddy, Mitochondria are a direct site of a beta accumulation in alzheimer's disease neurons: implications for free radical generation and oxidative damage in disease progression, Hum. Mol. Genet. 15 (9) (2006) 1437–1449.
[54] L. Morelli, R.E. Llovera, I. Mathov, L.F. Lue, B. Frangione, J. Ghiso, E.M. Castano, Insulin-degrading enzyme in brain microvessels: proteolysis of amyloid {beta} vasculotropic variants and reduced activity in cerebral amyloid angiopathy, J. Biol. Chem. 279 (53) (2004) 56004–56013.
[55] J. Apelt, K. Ach, R. Schliebs, Aging-related down-regulation of neprilysin, a putative beta-amyloid-degrading enzyme, in transgenic tg2576 alzheimer-like mouse brain is accompanied by an astroglial upregulation in the vicinity of beta-amyloid plaques, Neurosci. Lett. 339 (3) (2003) 183–186.
[56] Y.L. Chen, L.M. Wang, Y. Chen, J.Y. Gao, C. Marshall, Z.Y. Cai, G. Hu, M. Xiao, Changes in astrocyte functional markers and beta-amyloid metabolism-related proteins in the early stages of hypercholesterolemia, Neuroscience 316 (2016) 178–191.
[57] N.D. Belyaev, K.A. Kellett, C. Beckett, N.Z. Makova, T.J. Revett, N.N. Nalivaeva, N.M. Hooper, A.J. Turner, The transcriptionally active amyloid precursor protein (app) intracellular domain is preferentially produced from the 695 isoform of app in a {beta}-secretase-dependent pathway, J. Biol. Chem. 285 (53) (2010) 41443–41454.
[58] K. Sato, C. Tanabe, Y. Yonemura, H. Watahiki, Y. Zhao, S. Yagishita, M. Ebina, S. Suo, E. Futai, M. Murata, S. Ishiura, Localization of mature neprilysin in lipid rafts, J. Neurosci. Res. 90 (4) (2012) 870–877.
[59] D. Yui, Y. Nishida, T. Nishina, K. Mogushi, M. Tajiri, S. Ishibashi, I. Ajioka, K. Ishikawa, H. Mizusawa, S. Murayama, T. Yokota, Enhanced phospholipase a2 group 3 expression by oxidative stress decreases the insulin-degrading enzyme, PLoS One 10 (12) (2015) e0143518.
[60] E.S. Song, D.W. Rodgers, L.B. Hersh, Insulin-degrading enzyme is not secreted from cultured cells, Sci. Rep. 8 (1) (2018) 2335.
[61] M.L. Liu, M.P. Reilly, P. Casasanto, S.E. McKenzie, K.J. Williams, Cholesterol enrichment of human monocyte/macrophages induces surface exposure of phosphatidylserine and the release of biologically-active tissue factor-positive microvesicles, Arterioscler. Thromb. Vasc. Biol. 27 (2) (2007) 430–435.
[62] K. Strauss, C. Goebel, H. Runz, W. Mobius, S. Weiss, I. Feussner, M. Simons, A. Schneider, Exosome secretion ameliorates lysosomal storage of cholesterol in niemann-pick type c disease, J. Biol. Chem. 285 (34) (2010) 26279–26288.
[63] A. Hafiane, J. Genest, Atp binding cassette a1 (abca1) mediates microparticle formation during high-density lipoprotein (hdl) biogenesis, Atherosclerosis 257 (2017) 90–99.
[64] M. Colombo, G. Raposo, C. Théry, Biogenesis, secretion, and intercellular interactions of exosomes and other extracellular vesicles, Annu. Rev. Cell Dev. Biol. 30 (1) (2014) 255–289.
[65] G. Minakaki, S. Menges, A. Kittel, E. Emmanouilidou, I. Schaeffner, K. Barkovits, A. Bergmann, E. Rockenstein, A. Adame, F. Marxreiter, B. Mollenhauer, et al., Autophagy inhibition promotes snca/alpha-synuclein release and transfer via extracellular vesicles with a hybrid autophagosome-exosome-like phenotype, Autophagy 14 (1) (2018) 98–119.
[66] U. Sengupta, A.N. Nilson, R. Kayed, The role of amyloid-beta oligomers in toxicity, propagation, and immunotherapy, EBioMedicine 6 (2016) 42–49.
[67] M.D. Ledesma, J.S. Da Silva, K. Crassaerts, A. Delacourte, B. De Strooper, C.G. Dotti, Brain plasmin enhances app alpha-cleavage and abeta degradation and is reduced in alzheimer's disease brains, EMBO Rep. 1 (6) (2000) 530–535.
[68] H.M. Tucker, J. Simpson, M. Kihiko-Ehmann, L.H. Younkin, J.P. McGillis, S.G. Younkin, J.L. Degen, S. Estus, Plasmin deficiency does not alter endogenous murine amyloid beta levels in mice, Neurosci. Lett. 368 (3) (2004) 285–289.
[69] B.C. Miller, E.A. Eckman, K. Sambamurti, N. Dobbs, K.M. Chow, C.B. Eckman, L.B. Hersh, D.L. Thiele, Amyloid-beta peptide levels in brain are inversely correlated with insulysin activity levels in vivo, Proc. Natl. Acad. Sci. U. S. A. 100 (10) (2003) 6221–6226.
[70] N. Iwata, S. Tsubuki, Y. Takaki, K. Shirotani, B. Lu, N.P. Gerard, C. Gerard, E. Hama, H.J. Lee, T.C. Saido, Metabolic regulation of brain abeta by neprilysin, Science 292 (5521) (2001) 1550–1552.
[71] M.A. Leissring, W. Farris, A.Y. Chang, D.M. Walsh, X. Wu, X. Sun, M.P. Frosch, D.J. Selkoe, Enhanced proteolysis of beta-amyloid in app transgenic mice prevents plaque formation, secondary pathology, and premature death, Neuron 40 (6) (2003) 1087–1093.
[72] S.M. Huang, A. Mouri, H. Kokubo, R. Nakajima, T. Suemoto, M. Higuchi, M. Staufenbiel, Y. Noda, H. Yamaguchi, T. Nabeshima, T.C. Saido, et al., Neprilysin-sensitive synapse-associated amyloid-beta peptide oligomers impair neuronal plasticity and cognitive function, J. Biol. Chem. 281 (26) (2006) 17941–17951.
[73] C. Cornelius, R. Perrotta, A. Graziano, E.J. Calabrese, V. Calabrese, Stress responses, vitagenes and hormesis as critical determinants in aging and longevity: mitochondria as a "chi, Immun. Ageing 10 (1) (2013) 15.
[74] A. Trovato Salinaro, M. Pennisi, R. Di Paola, M. Scuto, R. Crupi, M.T. Cambria, M.L. Ontario, M. Tomasello, M. Uva, L. Maiolino, E.J. Calabrese, et al., Neuroinflammation and neurohormesis in the pathogenesis of alzheimer's disease and alzheimer-linked pathologies: modulation by nutritional mushrooms, Immun. Ageing 15 (8) (2018).
[75] V. Pilipenko, K. Narbute, I. Amara, A. Trovato, M. Scuto, J. Pupure, B. Jansone, J. Poikans, E. Bisenieks, V. Klusa, V. Calabrese, Gaba-containing compound gammapyrone protects against brain impairments in alzheimer's disease model male rats and prevents mitochondrial dysfunction in cell culture, J. Neurosci. Res. 97 (6) (2019) 708–726.
[76] R. Chillemi, N. Cardullo, V. Greco, G. Malfa, B. Tomasello, S. Sciuto, Synthesis of amphiphilic resveratrol lipoconjugates and evaluation of their anticancer activity towards neuroblastoma sh-sy5y cell line, Eur. J. Med. Chem. 96 (2015) 467–481.
[77] V. Calabrese, A. Santoro, A. Trovato Salinaro, S. Modafferi, M. Scuto, F. Albouchi, D. Monti, J. Giordano, M. Zappia, C. Franceschi, E.J. Calabrese, Hormetic approaches to the treatment of Parkinson's disease: perspectives and possibilities, J. Neurosci. Res. 96 (10) (2018) 1641–1662.